# Energy Efficiency of Radio Units and its Impact on RAN Energy Consumption

Master's Thesis in Electrical Measurements

Thomas Berglund
Helen Huynh

Ericsson AB
Department of Biomedical Engineering, Lund University
Faculty of Engineering LTH

Supervisors: Jonas Bengtsson and Johan Nilsson

Examiner: Lars Wallman

2017

Printed in Sweden
Tryckeriet i E-huset, Lund

# Abstract

As mobile telecommunications networks continue to grow, energy consumption continues to grow with it. This will without a doubt affect both the operational expense for network operators and the environment due to air pollution from power stations. As of today, a lot of radio units are consuming more power than necessarily, and with the growing industry this will have a substantial impact in the future. One way to address this issue is to make radio units more energy efficient. To approach this a study on Radio 2217, an Ericsson remote radio unit, was conducted. The study involved work on both hardware and software level. In order to test and evaluate the results a real LTE radio base station was set up. An LTE network was also modeled in Matlab with the purpose to show how different power save features of radio units could reduce the energy consumption. The findings of this work shows that the existing power save implementations of the radio unit could definitely be improved. The power save features Cell-Sleep and MIMO-Sleep were improved by 36 % and 3.4 % respectively. It also showed that the energy consumption in a mobile network could be reduced by up to 57 % by modernizing hardware and adding power save features.

# Preface

This thesis work was done at Ericsson in Lund in order to investigate if modern radio units could be made more energy efficient and also to highlight the impact that power save features has on the energy consumption by modeling a realistic network.

We would like to thank everyone at Ericsson in Lund, Kista and Ottawa who has helped us during our thesis work. Thanks to everyone at the office who has been very helpful and endured our questions about everything from hardware configurations to theory and a special thank you to our supervisor Jonas Bengtsson who always was there to discuss and guide us in the right direction. We would also like to thank our supervisor Johan Nilsson at Lund Institute of Technology and finally we would like to thank friends and family who has supported us during our studies and always being there for us.

Thank you,
Thomas Berglund & Helen Huynh

# Popular Science Summary

During the last decades, mobile networks have continued to grow and are expected to grow even further with the introduction of Internet of Things and the next generation radio system named 5G. As the networks grow, energy efficiency and sustainability is becoming more and more interesting and necessary for the network operators. However, energy efficiency is an area often overlooked in favor of connectivity, throughput and availability when building mobile networks.

To see how we could increase the energy efficiency of radio units we studied both hardware and existing energy efficiency features to see if there were any possibilities to improve the current implementations. Due to our time limit we quickly realized we could not do any hardware changes in the means of changing components for more efficient ones, for example by introducing more efficient transistors in the power amplifier. Instead, our focus became trying to improve the current power save features that were implemented in the radio. We focused mainly on two features, one which during low traffic scenarios turns off one of the transmitter branches to save power, and one feature that basically powers down the radio when there is no need for the radio to transmit nor receive.

The focus on the features became trying to turn off excess components that were not used, but still powered on and consuming power. To do this we set up a complete end-to-end system with real mobile phones connected to a real base station which was based LTE technology. This gave us full control over the system to test the features and to control the radio unit.

A novel approach used to identify components that were consuming power was to look at the circuit board with a thermal camera to find "hot spots", i.e. components that were consuming power. This helped us identify what we should focus on and proved to be good at visualizing the results. By the end of our work we managed to reduce the power consumption in the features by 36 % and 3.4 % respectively. We also created a model to show how new hardware and activation of power save features impacted the energy consumption of a realistic LTE network. It is shown in the model that by replacing old hardware by new modern hardware and activating and using power save features more often, the energy consumption can be reduced by up to 57 %.

# Table of Contents

# Abbreviations

| | |
|---|---|
| **3GPP** | Third Generation Partnership Project |
| **AIB** | Antenna Interface Board |
| **ASIC** | Application-specific Integrated Circuit |
| **ADC** | Analog to Digital-Converter |
| **BB** | Baseband |
| **CAPEX** | Capital Expenditure |
| **CP** | Cyclic Prefix |
| **CRS** | Cell-specific Reference Signals |
| **CPRI** | Common public radio interface |
| **DAC** | Digital to Analog-Converter |
| **DPD** | Digital Pre-Distortion |
| **DRX** | Discontinuous Reception |
| **DSP** | Digital Signal Processor |
| **eNB** | Evolved NodeB |
| **E-UTRA** | Evolved Universal Mobile Telecommunications System |
| **FFT** | Fast Fourier Transform |
| **FDD** | Frequency-Division Duplex |
| **HOPE** | Headroom Optimized Power Enhancements |
| **ITK** | In Service Performance Tool Kit |
| **IFFT** | Inverse Fast Fourier Transform |
| **KS/s** | 1000 samples per second |
| **LNA** | Low Noise Amplifier |
| **LTE** | Long Term Evolution |
| **LTU** | Local Time Unit |
| **MIMO** | Multiple Input Multiple Output |
| **MISO** | Multiple Input Single Output |
| **OFDM** | Orthogonal Frequency-Division Multiplexing |
| **OPEX** | Operating Expenditure |
| **PSF** | Power Save Features |
| **PA** | Power Amplifier |
| **PCB** | Printed Circuit Board |
| **PRB** | Physical Resource Block |

| | |
|---|---|
| **QAM** | Quadrature Amplitude Modulation |
| **RAN** | Radio access network |
| **RBS** | Radio base station |
| **RE** | Resource element |
| **RF** | Radio frequency |
| **Rx** | Receiver |
| **SAW filter** | Surface acoustic wave filter |
| **SIMO** | Single Input Multiple Output |
| **SISO** | Single Input Single Output |
| **TCO** | Total Cost of Ownership |
| **TDD** | Time-Division Duplex |
| **TDMA** | Time-Division Multiple Access |
| **TMA** | Tower Mounted Amplifier |
| **TOR** | Transmit observation receiver |
| **TRX** | Transceiver |
| **TTMF** | Triple Tower Mounted Filter |
| **Tx** | Transmitter |
| **UE** | User equipment |
| **VSWR** | Voltage Standing Wave Ratio |

# Chapter 1
# Introduction

As network traffic continues to grow, energy efficiency and sustainability will become even more important, especially for mobile network operators. Over the past 5 years mobile data traffic has grown 18-fold. With the introduction of smart phones and tablets as well as other connected devices, the load on mobile networks has continuously risen. More than half of the traffic today in mobile networks comes from video streaming. [1]. The number of connected devices will continue to grow with the advancements made in Internet-of-Things (IoT) and Machine-type communication (MTC). It is estimated that by 2021 there will be over 28 billion connected devices compared to today's 20 billion [2].

Increased traffic also means increased power consumption and with it comes environmental as well as monetary effects. The gain with improving energy efficiency is therefore to reduce the environmental impact and to contribute with cost reductions.

In this thesis work LTE systems have solely been studied, even though there are a lot of systems that run mixed-mode carriers where LTE, W-CDMA and GSM coexist at the same time.

The purpose of this thesis is to increase energy efficiency of one of Ericsson's remote radio units, Radio 2217 which is a macro radio. The thesis can be seen as a continuation from a previously conducted thesis work at Ericcson aimed at optimizing energy performance of a micro radio unit. This thesis work will also aim to show how power save features affects an entire network with aspects on both Total Cost of Ownership (TCO) but also the impact it has on the environment. This means that the functions of the radio will be studied as well as its existing power save features. A model for calculating the energy consumption with different types of radios will also be created.

This report will begin by presenting background theory of mobile communication, existing power save features and measurements. It then continues with an inter-working description of the radio unit this thesis was based upon in Chapter 3. After follows how the network was modeled in Chapter 4. In Chapter 5 methodology is presented and results are presented in Chapter 6, followed by discussion and conclusion in Chapter 7 and 8.

# Chapter 2
# Theory

This chapter will present theory behind how mobile telecommunication works. It will describe the LTE architecture, some existing power save features, theory behind the measurement setup and a brief introduction of the energy model.

## 2.1 Mobile telecommunications

Mobile telecommunication is a wireless communication system that enables communication between mobile devices. It typically exists of a core network that is connected to a radio access network (RAN) that wirelessly handles the communication between connected devices.

The evolution of mobile telecommunications, see Table 2.1, has developed steadily since the 80's. 5G (NR) is still being developed in time of writing and no standard has been set yet. The first generation (1G) was based on analog technology and used for voice-communication. The second generation (2G) appeared in the beginning of the 90's and the technology then switched to being digital instead. With the new technology that was based on Time Division Multiple Access (TDMA) it became possible to allow more users. With this technology higher transmission rates were obtained. It was also at that time the use of the text function Short Message Service, SMS, became available. The third generation offered even higher data rates and enabled more features such as multimedia and mobile broadband services [3].

**Table 2.1:** Evolution of Mobile telecommunication with highest achieved data rate

| Generation | Multiplex | Data rate | Introduction Year |
|---|---|---|---|
| 1G (NMT) | FDMA | - | 1984 |
| 2G (GSM) | TDMA/CDMA | 14.4 kbps | 1991 |
| 2.5G (GPRS) | TDMA/CDMA | 144 kbps | 1995 |
| 3G | CDMA | 2 Mbps | 2001 |
| 3.5G | WDCMA | 28 Mbps | 2002 |
| 4G (LTE) | MIMO-OFDM | 1 Gbps | 2010 |
| 5G (NR) | To be decided | Several Gbps | 2020 |

## 2.2 Long Term Evolution (LTE)

The demands for faster mobile broadband and better data capacity were among the main reasons to develop from 3G technology. The purpose of the development from 3G to 4G was to obtain:

- Increased performances such as data rate and bandwidth efficiency
- Wider network spectrum and low transmitting power
- Larger support for different applications and platforms such as digital TV and streaming of video
- Lower costs
- Lower latency

Amongst the improvements accomplished since 3G was a higher bandwidth efficiency using Orthogonal Frequency-Division Multiplexing (OFDM) in the downlink (DL) and Discrete Fourier Transform Spread-OFDM (DFTS-OFDM) in the uplink (UL), and bandwidth up to 20 MHz. The modulation techniques used are QPSK, 16 QAM, 64 QAM and 256 QAM [4], [5].

The other 4G-standard is LTE-Advanced which is the evolution of former LTE versions. With the aims to obtain wider bandwidths, higher peak data rates and reduced latency etc. the new 4G standard had several technologies implemented such as Carrier Aggregation (CA), Multiple-Input Multiple-Output (MIMO), Coordinated Multi-Point (CoMP) and Relaying [4].

### 2.2.1 Fundamentals of LTE Architecture

This subsection explains the fundamentals of LTE architecture to provide a better understanding of how the system is built and interconnected. The part interesting to this thesis work is the radio access network (RAN) and radio base stations in particular. Radio base stations are explained further in Section 2.2.2.

The LTE architecture consists of the Evolved Packet Core (EPC) and the RAN which is called E-UTRAN. The EPC is part of the System Architecture Evolution (SAE) in 3GPP's standard for LTE. It is an evolution of the old GSM/GPRS circuit switched networks to a fully packet-switched system. The EPC makes up the core network and consists of several types of nodes illustrated in Figure 2.1 [6].

The Serving Gateway (S-GW) is the node responsible for connecting the EPC to the LTE RAN. The Packet Data Network Gateway (P-GW) is responsible for connecting the EPC to the Internet. The Mobility Management Entity (MME) manages connections and releases of bearers to a user equipment (UE) and other UE related functions. The Home Subscriber Service (HSS) node contains subscriber information for the network. The EPC also contains other nodes such as

The Policy Control and Charging Rules Function (PCRF) [6],[7].

The RAN consists of eNodeBs which are responsible for all radio-related functions. In LTE, the eNodeB is a logical node which means that it can be a physical implementation but it does not have to be. One common implementation of the eNodeB, and the implementation used in this thesis work for the model (see Chapter 4), is a 3-sector implementation [7].

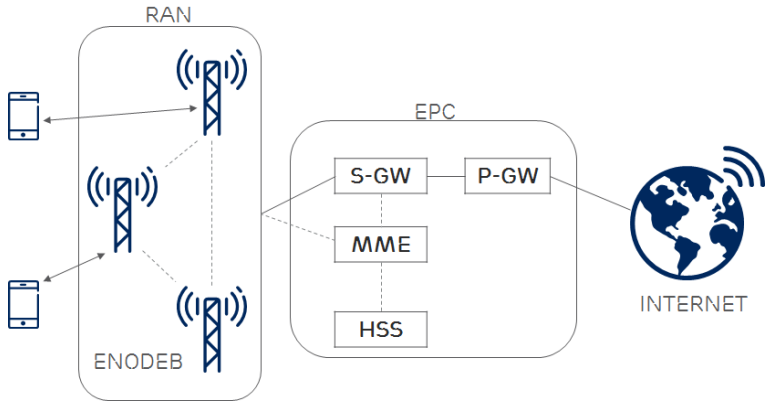


**Figure 2.1:** Overview of LTE architecture.

### 2.2.2 Radio Base Station (RBS)

The deployment of a modern radio base station in LTE is a three-sector cell with three antennas and three radios, making up three 120° sectors. An illustration is shown in Figure 2.2 and a real example can be seen in Figure 2.3. The cabinet usually contain a baseband, batteries and climate control. The baseband (BB), or digital unit, is a multi-core processing unit which is responsible for decoding uplink and downlink radio signals, radio control processing, network synchronization and IP interface [8].

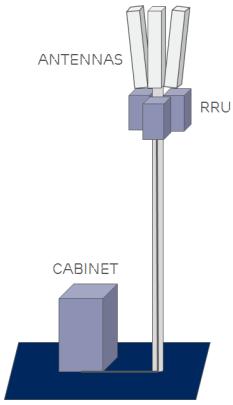


**Figure 2.2:** Illustration of a three-sector radio base station with a cabinet containing baseband, batteries and climate control. In Figure 2.3 an Ericsson RBS is shown.

**Figure 2.3:** Ericsson 3-sector RBS with cabinet enclosure to the left containing baseband, batteries and climate control. Right side shows three antennas with 3 remote radio units.

### 2.2.3 Orthogonal Frequency-Division Multiplexing (OFDM)

OFDM is a modulation technique that allows several signals to be transmitted simultaneously within an OFDM signal interval $T_s$. The technique provides several advantages, with bandwidth efficiency as one of them. An OFDM-signal consists of the sum of numerous different QAM-signals, each with its own carrier frequency. The number of QAM-signals in an OFDM-signal vary, is usually between a couple of hundred to a couple of thousand. Before transmitting the OFDM-signal a cyclic prefix (CP) is added at the beginning. This parameter is of great importance since a well-designed CP helps to deal with the issues of inter-symbol interference at the receiver side [9].

Thanks to the sub-carrier frequency separation $f_\Delta$, being;

$$f_\Delta = 1/T_{obs} \tag{1}$$

where $T_{obs}$ is the observation interval of the receiver, all the QAM-singals in the received OFDM-signal can be orthogonal which makes it easy for the receiver to identify them even when they are overlapping each other. Furthermore, an important rule is that the duration of the CP should be at least equal or longer than the duration of the impulse response of the channel in order to keep orthogonality between the channels [10].

### 2.2.4 LTE Time Domain Structure

In LTE, the time domain is structured as frames which are then broken down into symbols. As can be seen in Figure 2.4, a frame is 10 ms and consists of 10 sub frames. Each sub frame consists of two slots, which are 0.5 ms each. Each slot is then divided into 7 symbols in the case of normal CP. With the extended CP each slot consists of 6 symbols [7].

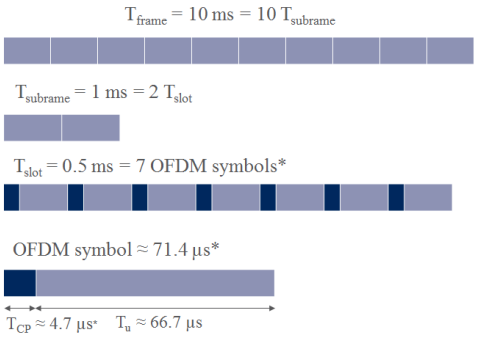


**Figure 2.4:** Time domain structure for normal cyclic prefix.
*6 symbols and 83.4 $\mu$s in the case of extended cyclic prefix.

### 2.2.5 LTE Downlink Time-Frequency Grid

In LTE, time and frequency can be understood as a grid of resource elements (RE). The grid consists of Physical Resource Blocks (PRB) which are made up of 12 sub-carriers over seven OFDM symbols. A Resource Block pair consists of two PRB after one another in the time domain, covering 14 OFDM symbols. The minimum LTE bandwidth consists of six PRB. A RB pair has 168 resource elements, some of which are occupied by Cell-specific Reference Signals (CRS) signaling and control signaling. The CRS are used for channel estimation and are crucial for the UE to demodulate the channels coherently.

In Figure 2.5 the LTE Time-Frequency grid is shown with added CRS and control region for two transmit antennas. The number of CRS signals are reduced with fewer antennas and increased with more antennas. The empty resource elements

are used to carry data. If there are no data to be sent, the symbols will be empty [7].

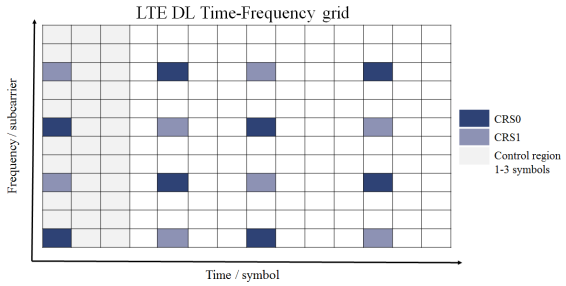


**Figure 2.5:** LTE time-frequency grid with CRS symbols for two antennas. Resource elements in white are used to carry data.

### 2.2.6 LTE Uplink Time-Frequency Grid

Compared to the downlink time-frequency grid, the uplink grid transmits its control signals in the Physical Uplink Control Chanel (PUDCCH) at the edges of the bandwidth, covering all OFDM symbols. The data is sent around the center of the bandwidth in the Uplink Shared Channel (UL-SCH). Also covering all subframes is the Physical Random Access Channel (PRACH) [7]. The time-frequency grid can be seen in Figure 2.6.

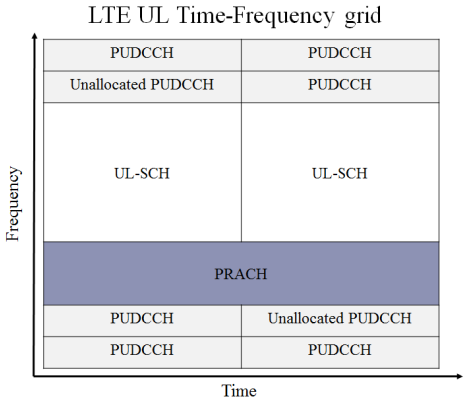


**Figure 2.6:** LTE time-frequency grid for uplink.

### 2.2.7 MIMO - Multiple-Input Multiple-Output

MIMO is a method for increasing the capacity of a radio transmission channel with the use of multiple transmit and receive antennas [11]. By using multiple antennas

at both transmitter and receiver side several benefits can be obtained, such as Spatial Multiplexing and Spatial Diversity [12]. Spatial multiplexing is accomplished by transmitting independent data simultaneously from each transmit antenna, in the same frequency band. This increases the capacity linearly with the number of antennas, and therefore also increases the bandwidth efficiency[9]. Spatial Diversity is accomplished by transmitting the same data over multiple independent channels. The purpose is then that hopefully at least one of the signals will survive, since the fading in each channel is independent of the others. This results in an improved link-reliability with lower bit error probability and also reduced co-channel interference [7], [8]. An illustration of MIMO is given in Figure 2.7. The combination of MIMO and OFDM has had significant improvements in LTE with regards to data rate and link reliability.

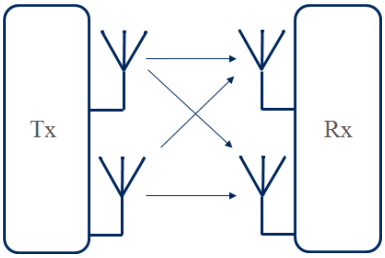


**Figure 2.7:** In MIMO, signals can be transmitted in different ways to achieve either spatial multiplexing or spatial diversity.

### 2.2.8 Frequency-Division Duplexing (FDD) & Time-Division Duplexing (TDD)

LTE has support for both Frequency-Division Duplex and Time-Division Duplex, see Figure 2.8 and Figure 2.9, enabling spectrum flexibility by having the ability to operate in both paired and unpaired spectrum.

In FDD, different carrier frequencies are used for uplink and downlink transmissions, giving the name Frequency-Division. The uplink and downlink transmissions are sent in frames which are discussed in sections 2.2.3-2.2.5. With the use of FDD, the RBS or the UE can both receive and transmit simultaneously, given that the device supports full-duplex transmission. Full-duplex devices requires a more complex device implementation but enables higher data rates [7]. FDD requires generally twice the amount of spectrum compared to TDD, but enables lower latency.

In TDD, uplink and downlink operate at the same carrier frequency leading to the transmissions having to be separated in time, hence the name Time-Division. The uplink and downlink transmissions are allocated in different time slots where downlink transmissions only can occur in downlink time slots and vice versa. The distribution of uplink and downlink time slots can be varied to account for traffic

needs. Although TDD can effectively allocate traffic resources where needed, this duplex scheme may have a negative impact in terms of latency. Because both uplink and downlink use the same carrier frequency the RBS and UEs have to switch between uplink and downlink transmission continuously [7].

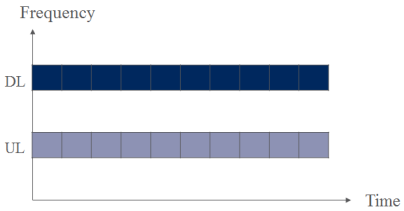


**Figure 2.8:** FDD

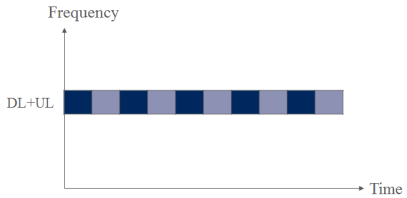


**Figure 2.9:** TDD

### 2.2.9 Frequency Bands

In LTE there are a lot of different frequency bands in use. The available frequency bands differ from country to country because of regional differences in available spectrum and laws. Some frequency bands provide different functionality compared to others, depending on the frequency of the band. Comparing Band 1 (2100 MHz) with Band 8 (900 MHz), see Figure 2.10, we note that band 1 has shorter coverage than band 8, which is due to the higher frequencies causing propagation loss. Since lower frequencies have less penetration loss the signals can travel further and therefore provide better coverage. The propagation loss can be verified by Friis Transmission Equation.

$$\frac{P_r}{P_t} = G_t G_r (\frac{\lambda}{4\pi R})^2 \tag{2}$$

Where $P_r$ is received power, $P_t$ is transmitted power, $G_t$ transmitter gain, $G_r$ receiver gain, $\lambda$ the wavelength and $R$ the distance between antennas. For this reason, bands at lower frequencies are better suited for rural deployment while bands at higher frequencies are more suited for urban areas.

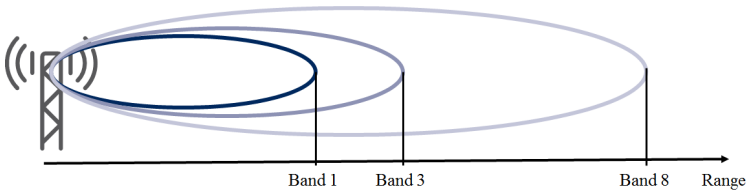


**Figure 2.10:** Differences in coverage range by using different frequency bands. The higher the frequency of the band the shorter the range due to propagation losses.

## 2.3 Power save features

In this section several existing power save features will be presented. The thesis will aim to improve some of the features and all of them are to be included in the model to show how they affect the energy consumption in a mobile network.

### 2.3.1 Cell Sleep

Cell Sleep is a mode in which the radio neither sends downlink data or receives uplink data. Several components can be powered down during the sleep time and the only way to communicate with the radio is through the CPRI (Common Public Radio Interface) connection which is connected between the baseband unit and the radio. This feature can be used to deactivate a cell that is only used as a capacity cell when the load on it is low. An example could be a RBS at a sports stadium which requires high capacity during events but sees low load otherwise. The concept is illustrated in Figure 2.11 and Figure 2.12. At the moment there is a shift from what is called "always on" to "always available", which means that capacity cells should be turned off when they are not needed.

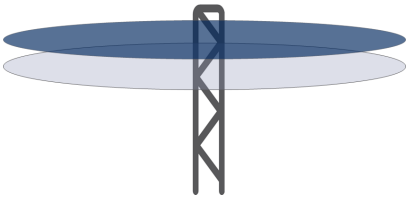

**Figure 2.11:** Both capacity cell and coverage cell are enabled.

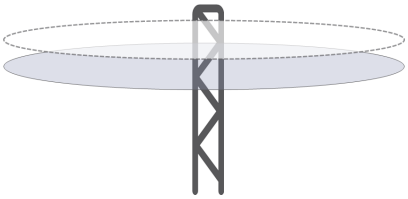

**Figure 2.12:** Capacity cell put to Sleep.

### 2.3.2 MIMO-Sleep

MIMO-Sleep is a power save feature where the radio changes operation from MIMO to SIMO (Single-Input Multiple-Output) by shutting off one of the TX-branches, mainly the power amplifier (PA) component. The feature is currently configured to activate during low load-scenarios, typically during night time. By turning off a TX-branch the radio saves power, however, at the cost of decreased diversity, spatial multiplexing and coverage in downlink [13].

### 2.3.3 Micro-Sleep TX

The Micro-Sleep TX feature works by shutting down the PA on both chains during LTE symbol times that are not scheduled to carry any data, control or reference signaling. The feature lowers the power consumption the most at low loads and shows no savings at full load due to the inability to turn off the PA since all symbols are occupied. Lowers the overall power consumption without degrading network performance [13].

### 2.3.4 LESS - Low Energy Scheduler Solution

LESS schedules the incoming data in a way that they are put in a buffer and sent together in chunks rather than in separate blocks. This leads to more available symbol times in which Micro-Sleep Tx can be used more frequently. It also enables the use of higher modulation since more data is scheduled during fewer symbol times [13].

### 2.3.5 HOPE - Headroom Optimized Power Enhancements

HOPE increases the PA efficiency by changing the level where the PA overloads and thus clips the signal such that the digital pre-distortion (DPD) and the PA uses the same clipping settings. HOPE lowers the power consumption during all loads [13].

### 2.3.6 PSI-Coverage ($\Psi$)

PSI-coverage gets its name from the similarity to the Greek letter $\Psi$ where a single remote radio unit (RRU) is connected to three antennas to form a three-sector site. The PSI-solution provides similar coverage and throughput in low load areas compared to a conventional three-sector site but with at least two less RRUs. This brings down the energy consumption by at least 40 percent. It is best suited for low to medium traffic sites [13].

## 2.4 Power measurements

To be able to supply and measure the power consumption of the radio accurately a four-wire sense setup, see Figure 2.13, was used between the power supply, a DC power analyzer (Keysight N6705B), and the radio. The radio was supplied with -48 V DC. Current is supplied via source leads. The source leads generate a voltage drop according to Ohm's law because of the impedance in the wires.

$$U = R \cdot I \tag{3}$$

The voltage drop equals the impedance in the wires multiplied by the current. To account for the voltage drop a pair of sense leads are attached to a voltage meter that measures the voltage at the source output. The source then adjusts the voltage accordingly to account for the voltage drop in the source wires. Because the sense wires are connected to a voltage meter, which has an impedance of around 10 M$\Omega$, virtually no current will flow in its direction resulting in a negligible voltage drop.

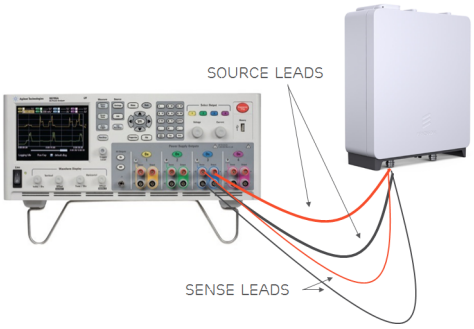


**Figure 2.13:** Four wire sense to accurately supply and measure power consumption. The voltage drop from the source leads is measured at the input to the radio.

## 2.5 Electric power and energy

Electric power is the rate of work done when an electrical current flow through a potential difference. It has the SI unit W (Watts) and its instantaneous electrical power is given by

$$P = U \cdot I \tag{4}$$

Where P is the instantaneous power measured in Watts, U is the potential difference in voltage and I is the current measured in amperes. Energy, on the other hand, is a measure of the work done over time. Energy is given by

$$Energy = power \cdot time \tag{5}$$

Where power often is given in kW (kilowatt) and time in hours. This gives kWh (kilowatt-hours) which is a common unit for energy, where 1 kWh equals 3.6 MJ.

## 2.6 Energy Model

The purpose of creating an energy model of a mobile telecommunication network is to be able to grasp what consumes power and in what way it does so. This can help in understanding what can be done to save power and give ideas of how to create a more energy efficient network. To model the power consumption in a network several assumptions have been made. Quadratic curves for the radios has been made by collecting power consumption data from live measurements and PowerCalc and using this to fit quadratic curves.

$$\text{Power consumption} = \alpha x^2 + \beta x + \delta \tag{3}$$

Where $\alpha$, $\beta$ and $\delta$ are coefficients received from the polynomial fitting of the power measurements, see Appendix C, and $x$ is the load for which the power consumption needs to be modeled. Even though the power consumption is fairly linear, a quadratic polynomial has been chosen to better account for the small variations during low loads in the radio [13].

### 2.6.1 Traffic and radio energy consumption

It has been shown that the LTE energy consumption only increases a few percentage with the increase of data traffic. An estimation of the traffic scenario for 2015 showed an power consumption increase of less than 2 % comparing with the network without data traffic. Even with the most extreme estimation of the traffic scenario the energy consumption only increased with 7.4 % [13].

To generalize the case for most radios today; typically there is a relatively high power consumption for when there is no or low load. The power consumption then increases rather linearly with increased load. Figure 2.14 illustrates the relation between power consumption and load. Cell-Sleep is when the radio can not transmit nor receive any data. Active is when the radio is idle and only transmitting control signaling. Full load is when the radio transmits with maximum capacity. This graph could be applied to most of the radios used today, as can be seen in Figure 2.15 which shows the actual case for Radio 2217.

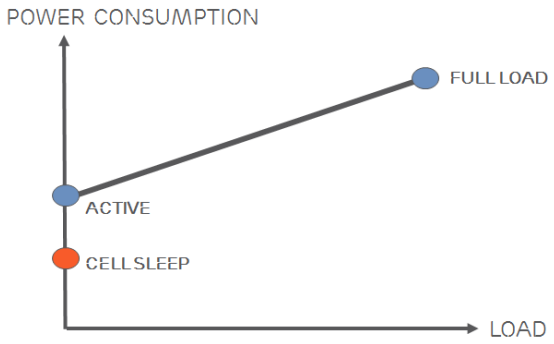


**Figure 2.14:** Illustrates power versus load. The power consumption during idle is not much less than during full load.

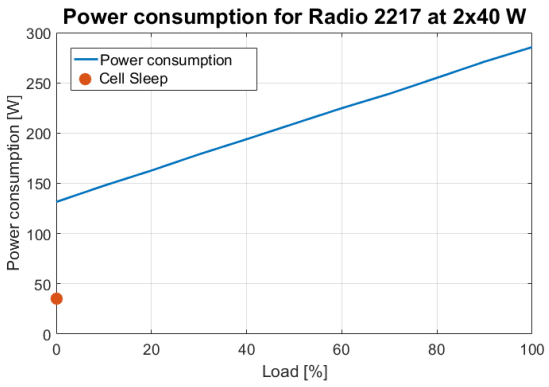


**Figure 2.15:** Shows power consumption versus load percentage for Radio 2217.

### 2.6.2 Off-grid sites and diesel consumption

Off-grid sites are sites that are not connected to the electrical power grid and thus have to rely on stand-alone power systems. Bad-grid sites are sites connected to the electrical grid but with high unreliability and often not good quality. These sites also rely on stand-alone power systems [14]. According to [15] the number of bad-grid and off-grid sites are expected to grow in developing countries in Africa and Asia from around 1 million today to 1.2 million in 2020. Out of this number, 31 % were off-grid 2014 and the share of off-grid sites is expected to grow to 33 % by 2020. As an example, with numbers from telecom market sizing in India [16], 17.8 % of towers are placed off-grid. Off-grid sites are today mainly powered by diesel generators which contributes to air pollution by emitting considerable amounts of greenhouse gases. Off-grid sites are typically placed in rural areas as shown in Figure 2.16.

One liter of diesel contains around 38.6 MJ energy, which equals around 10.7 kWh. [17]. However, that assumes an efficiency of 100 % ($\eta = 1$). The average efficiency of internal combustion power plants equals around $\eta = 0.33$ [18], which means one liter of diesel only provides 3.53 kWh. One liter of diesel produces 2.6 kg $CO_2$ [17]. This value will be used when calculating the $CO_2$ emissions in the energy model.

**Figure 2.16:** Radio base station placed in a rural area [13].

# Chapter 3
# Radio Inter-working Description

This chapter has been removed to protect the confidentiality of Ericsson radio products.

# Chapter 4
# Energy Model

The purpose of the model is to show what impact different power save features will have on a network with regards to energy consumption. It also aims to demonstrate how much energy a network consumes and why it is important to enable power save features, as well as show the importance of modernization of hardware with a focus on energy efficiency. Reducing the energy consumption in a network not only reduces the TCO by reducing the energy costs, but also contributes to reduce the overall environmental impact it has.

At first, the model will consist of four types of radios that are actually being used today. The different power save features are then added to each of the sites configurations and corresponding power consumptions will be calculated. The same procedure are then done for the model substituted with newer radio units. The total savings in terms of costs and the total savings in terms of $CO_2$ emissions are presented in the result section.

## 4.1 Assumptions and limitations

Due to issues with confidentiality and non-disclosures of network operators' data and statistics, almost all data in the model have been estimated. The data has been estimated with help from experts in the field. Also, in order to scale down the complexity of the energy model several assumptions had to be made. The following assumptions of the model network are listed below.

- The radios used in the network model only have radios used with LTE technology.
- The network will consist of four types of radios units.
- The radio types in the model only supports FDD.
- PRB utilization, ie. the percentage of utilized physical resource blocks, is considered the load unit.
- The load distribution is the same for all site configurations
- Only the power consumption from the radio units are included
- The cost of 1 kWh is assumed to be 1 SEK

- 17.8 % of the sites are assumed to be off-grid with diesel generators as stand-alone power supply with assumed efficiency of $\eta = 0.33$.

With no access to a real network and because we were unable to receive access to statistics for a real network, several features had to be estimated. The estimations are based on some lab results but mostly on expert opinions from people who have worked with the features at Ericsson. An example is the feature LESS, which still is being tested in a live network in South Korea, that could not be measured with the setup available to us since it works best with sporadic data and has only some effect when sending TCP streams at full throughput.

## 4.2 Load distribution

For the model we have used the same load distribution, see Figure 4.1, for all sites. It can be seen in the figure that the majority of the sites experience low loads. The load and distribution was collected from a network in Australia consisting of both suburban and urban areas [13]. This distribution can be applied in different environments, as can be seen in Figure 4.2 [19]. This mean that urban, sub-urban and rural areas all have sites with high and low load. Although the average load often is higher in urban areas than in rural, this model uses the same load and distribution for all sites. So it can be assumed all sites are located in the same geographical area. In our model the average load during a day on the sites varies between 5 % and 71 %.

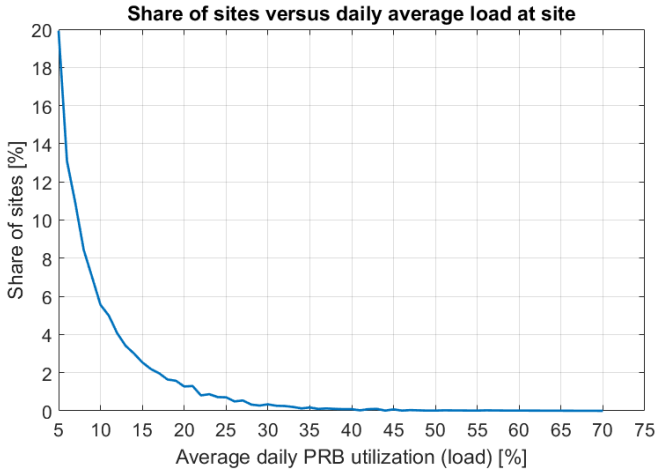


**Figure 4.1:** Load distribution used in the model.

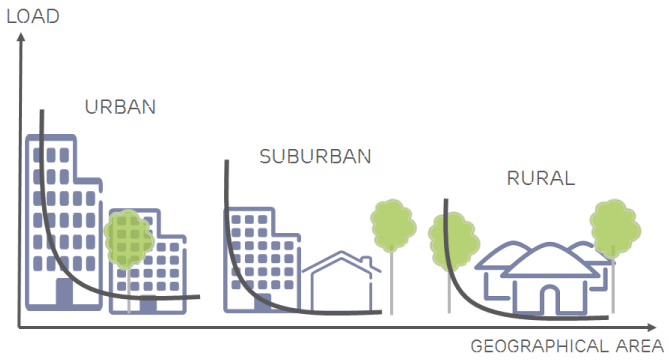


**Figure 4.2:** Figure shows how the load is distributed in different geographical areas.

## 4.3 Radios used in model

In the calculations seven different radio units have been used to account for the diversity in a real network, see Table 4.1. The radios operate on different bands to support both urban and rural deployments. The upgraded radios can substitute the older radios with same or better performance.

**Table 4.1:** Radios in model

| Site configuration | Existing radio | Upgraded radio |
|---|---|---|
| 1 | RRUS11 B1 & B5 | Radio 2219 B1 & Radio 2217 B5 |
| 2 | RRUS12 B1 & B8 | Radio 2219 B1 & Radio 2217 B8 |
| 3 | RUS02 B1 | Radio 2219 B1 |
| 4 | RRUS32 B3 | Radio 4415 B3 |

## 4.4 Site configuration

In the energy impact model a theoretical network in the region South East Asia & Oceania (RASO) is modeled. In this region the following E-UTRA (LTE) frequency bands are available: B1, B2, B3, B5, B7, B8, B28, B38, B40 and B44 [20]. The network consists of both rural (Band 5 and Band 8) and urban sites (Band 1 and Band 3). The site configurations can be seen in Table 4.2. Site configuration 1 and 2 has two bands available, resulting in six radios per site, whereas site configuration 3 and 4 only has one band available. Site configuration 3 uses a 1 TRX radio (RUS02 B1) and thus requires six to be able to support 2x2 MIMO. This configuration is substituted with Radio 2219 PSI-deployment. The substituted network model can be seen in Table 4.3.

The sites have been configured as three-sector sites with one radio per sector. Some of the sites have also been configured to have two frequency bands (one capacity band and one coverage band) to enable the use of Cell-Sleep.

**Table 4.2:** Model network - existing equipment

| Site configuration | Number of sites | Number of radios |
|---|---|---|
| 1 | 10 000 | 60 000 |
| 2 | 7000 | 42 000 |
| 3 | 5000 | 30 000 |
| 4 | 5000 | 15 000 |

**Table 4.3:** Model network - Upgraded equipment

| Site configuration | Number of sites | Number of radios |
|---|---|---|
| 1 | 10 000 | 60 000 |
| 2 | 7000 | 42 000 |
| 3 | 5000 | 5000 |
| 4 | 5000 | 15 000 |

## 4.5 Power consumption functions

As mentioned previously in section 2.4, the power consumption of the radios used in the model has been estimated by polynomial curve fitting to be able to calculate estimated power consumption at different loads. The coefficients used for all polynomials can be found in Appendix C.1. The coefficients were found by polynomial curve fitting from real measured values of several radio's power consumption at loads from 0 to 100 %. The data for Radio 2217 was measured by us in the lab, the other power consumption values were taken from PowerCalc, which uses real lab measurements made by Ericsson. The functions used are quadratic. In Figure 4.3 the power consumption for Radio 2217 can be seen when plotting the power consumption functions made with added power save features. In the figure Micro-Sleep Tx and LESS is used.

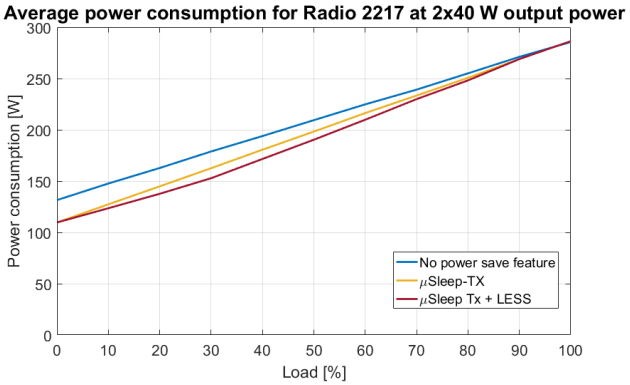


**Figure 4.3:** An example showing the effect power save features has on the power consumption.

## 4.6 Algorithms

In Appendix D, the different algorithms used in the model to calculate energy consumption for the network with different added power save features are presented. There are in total 6 different algorithms, where the first one, Algorithm 1, calculates the energy consumption with no power save features added. The last algorithm, Algorithm 6, calculates the energy consumption with all power save features added. Since the power save features are not additive, several polynomials had to be used in the different algorithms to enable the energy consumption to be calculated as realistically as possible.

### 4.6.1 Sleep estimations

When estimating how many hours during a day that MIMO-Sleep and Cell-Sleep could be activated Figure 4.4 was one of the graphs that was studied. In the figure the number of data radio bearer packets (DRB) received in uplink is plotted. The data was collected from a radio base station using a PSI-configuration [13]. Although it does not show the actual load percentage on the node, it gives an idea of how the traffic is distributed during the day. Similar graphs of other days were also studied and although they did not look the same some similarities could still be found. In all graphs there were periods of time where the so-called average load was low enough to consider activating some degree of sleep function. In this case it can be seen that between 01:00 and 09:00 the load is relatively low, and between 14:00 and 17:00 the load seems to be rather low as well.
Several proposals of how to configure the different sleep functions were made. Those are then applied for both the network before and after the hardware substitution in order to maintain the same conditions. Some of them are listed below.

- If the PRB utilization is below 12 %, then activate MIMO-Sleep for 10 hours of the day, otherwise only activate it for 3 hours.
- Sites with more than two bands should activate cell sleep on one of the bands

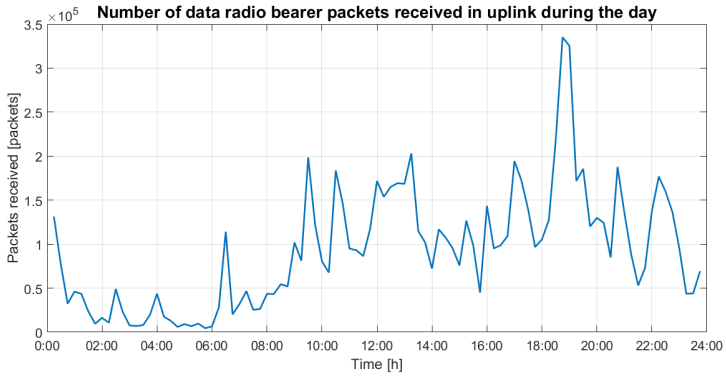


**Figure 4.4:** Average load during the day on an LTE site measured at 15 minute intervals.

for 6 hours if the PRB utilization is below 8 %, otherwise the algorithm for MIMO-Sleep is used.

- The power save features Micro-Sleep Tx, LESS and Hope are activated all the time.

The pseudo code in Appendix D explains further how the sleep estimations where configured.

# Chapter 5
# Methodology

This chapter presents the methodology used for investigating the possibility to reduce the power consumption of the radio. The first section presents the pre-study required to gain enough knowledge about the hardware. In the second section the measurement setup is presented with short explanations of the equipment used. Section three and four explains the methodology of investigating the radio opened and the investigation of power save features. The last section involves the methodology for creating the energy model.

## 5.1 Pre-study

The study began with collecting the documents needed for analyzing the radio unit. The datasheets, circuit diagrams and inter-working descriptions (IWD) were fetched from an internally developed database for hardware products. With the use of the circuit diagrams we were able to identify the blocks for transmission and reception, and with the datasheets of different components further analyzing of power consumption, wake-up times and other characteristics could be done.

Alongside with the study of documents we worked with a program for managing the radio by sending MO Shell commands, which is further explained in the sections below. When first studied, the radio was assembled. We quickly realized that, in order to study the radio further it had to be operated opened. This was an approach that usually is not considered so we had to order special radio antenna contacts, cables and a circuit card from the the Kista office. Since this was an unusual approach it took a long time to acquire the needed cables.

## 5.2 Measurement setup

The figure 5.1 below shows the lab equipment set-up. A CPRI cable was used as a communication link between the radio and the baseband. For measuring power consumption, the power analyzer Keysight N6705B, was connected to the radio's power cable using four-terminal sense to ensure correct measurements.

To be able to study and manipulate the different parts of the radio an internally developed software tool called MO Shell was used by sending shell commands to

the radio via the baseband unit. When different components were powered down tests were also made to see if there still was connection to the UEs. This was done using LiNS and iPerf. To be able to see which components were powered on a thermal camera was used. This was of course only possible if the radio unit was opened. A further description of how this was done can be found in the section below.

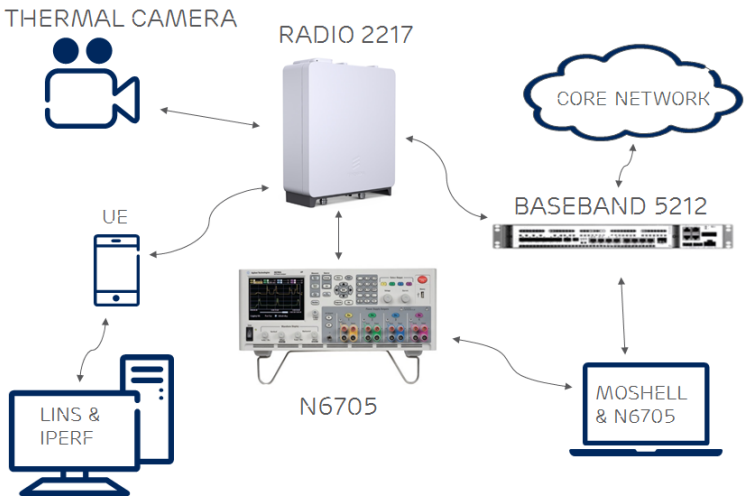


**Figure 5.1:** Measurement test set-up

### 5.2.1 Keysight N6705B

The Keysight N6705B DC power analyzer is an instrument that sources and measures DC voltage and current of the device. The built in voltmeter and ammeter makes it possible to measure and display power consumption. The inaccuracy of the measurements are up to 0.025 % with a sampling rate of up to 200 kHz.

### 5.2.2 MO Shell

To control the radio and the baseband a Managed Object (MO) shell was used. The radio's software was then accessed through a link-handler shell to be able to investigate different software commands on the radio. Several high level commands that were used had been implemented to control components.

### 5.2.3 Thermal Camera - FLIR P620

The thermal camera used in this thesis work was a FLIR P620 infrared camera. The camera has a thermal sensitivity of 40 mK at 30 °C and has a temperature range between -40 °C to 500 °C. The accuracy of the measurements are ±2°C or 2% [21]. The use of a thermal camera to identify components that were consuming power was very effective.

### 5.2.4 Iperf 3.11

To send data streams (TCP) to and from the UEs a command-line program called Iperf was used. It is a tool for measuring network performances such as throughput,jitter, data loss etc. In order to use Iperf two computers were needed, one of them acting as the client and the other one as the server. The client connects to the server you're testing the throughput of. In the setup for this thesis work, four UEs were connected to a computer running the program LiNS.

### 5.2.5 LINS

Lins is an internally developed tool used for network analysis such as observing RRC connection, RSRP values etc. To conduct communication with the UEs, AT commands were sent in each AT channel [13]. A brief summary of the commands used can be found in the Appendix B.

### 5.2.6 UE rack

The UEs used are real UEs that can receive and transmit data. The UEs are equipped with ST-Ericsson THOR M7450 LTE category 4 modem, capable of downlink and uplink data rates of up to 150 Mbps and 50 Mbps respectively [13].

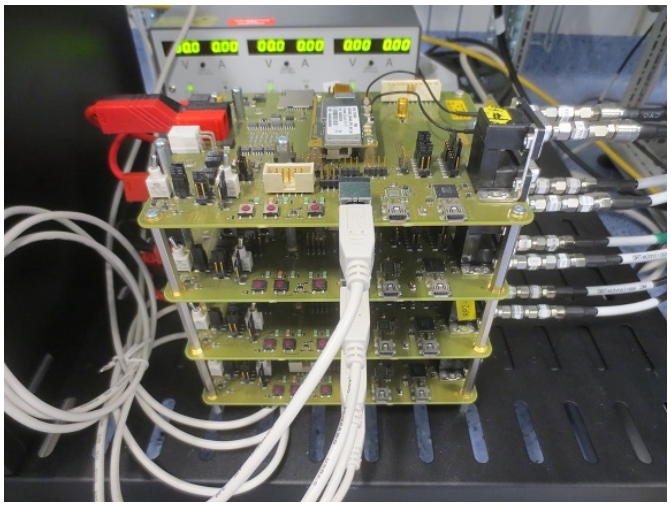

**Figure 5.2:** UE rack used when testing DL & UL data.

## 5.3 Operating the radio opened

To be able use the thermal camera to identify the components that were powered on and off during testing, we had to open up the radio and run it opened. To do this we had to order special antenna contacts, cables and a circuit card from the

office in Kista, Stockholm. The reason for this is that the radio's circuit board needs to be connected to the cavity filter in order to function. The circuit card is the connection between the circuit board and the filter unit on the cavity filter. To connect the filter unit we had to solder on a cable connecting the ordered circuit card to the existing circuit card we already had in the radio. The soldering of the cable to the circuit card can be seen in Figure 5.3. See Figure 5.4 for the complete setup.

The shields covering the TRX board and PA board were taken off to be able to use the thermal camera. Because of safety issues with radio frequency (RF) exposure we had to set the output power of the radio much lower than the actual output power, which is 2x40 W. Since we did not want to take any risks the output power was set to 1 mW.

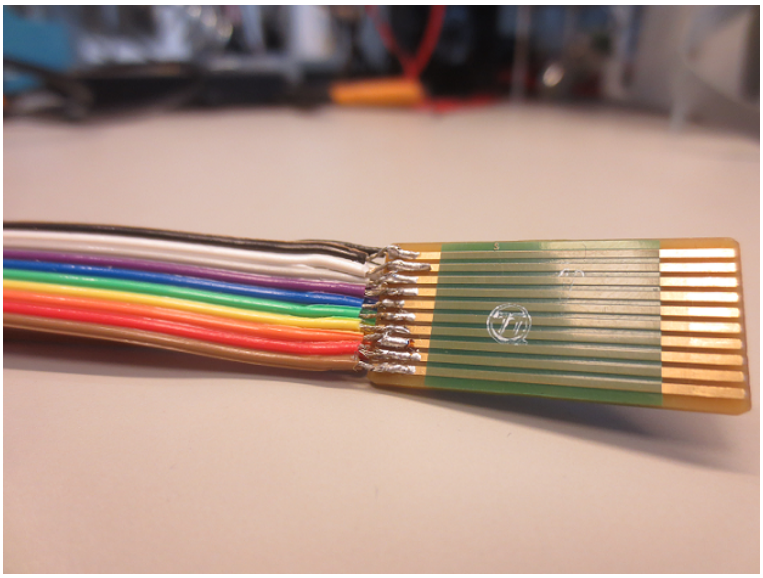

**Figure 5.3:** Photo of the soldering on the circuit card used to connect the boards.

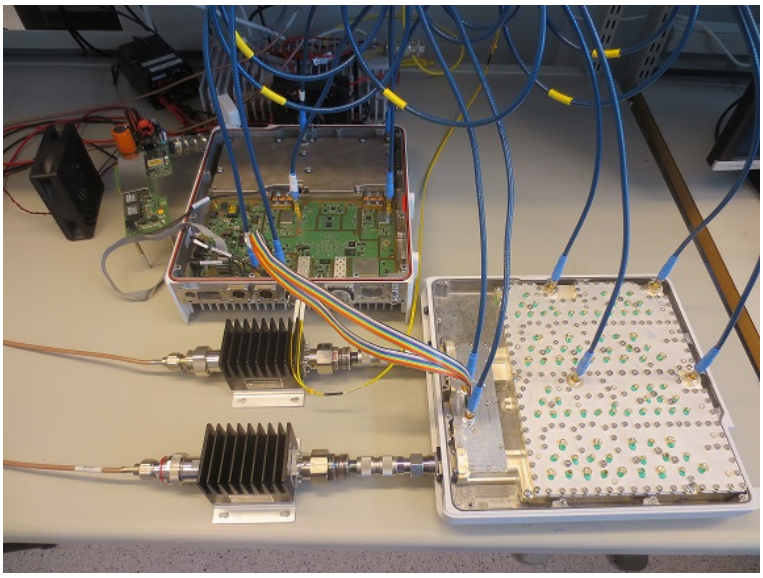

**Figure 5.4:** Shows how the radio was connected to the cavity filter with cables to be able to run it while opened.

### 5.3.1 Investigating hot spots

To find which components were powered on, a thermal camera was used. With the camera one could directly observe if a component was successfully powered down. As can be seen in Figure 5.5 and Figure 5.6, the heat dissipation from powered on components are easily visible.

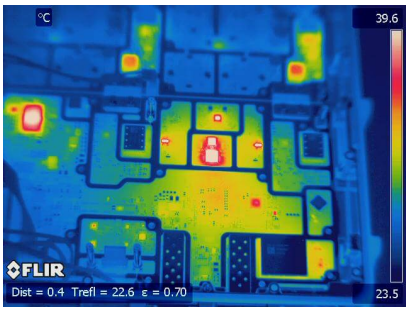


**Figure 5.5:** No CPRI connection to baseband

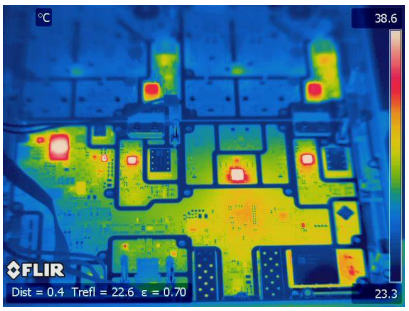


**Figure 5.6:** With CPRI connection to baseband

Figure 5.5 shows a thermal camera photo taken without the CPRI connected. Notice how the LNAs and receiver chain is on. In Figure 5.6 the CPRI has been connected and the image shows how some power save features already have been implemented. Notice that both modulator ASICs have been turned on.

## 5.4 Power save features

After having learned more about the radio and understood how to power down components with MO Shell, the next step was to look at the power save features that can be enabled. The main power save features the work was focused on were Cell-Sleep, MIMO-Sleep and Micro-Sleep Tx. To make sure our improvements were feasible it was made sure that the implementations did not cause any hardware faults or other alarms that could not be reset. Another test involved making sure that the components could be powered on again with the same results as before.

To control and power off components several shell scripts were written. The shell scripts contained both high level commands already implemented in the radio's software and SPI-commands. The way to configure each component with SPI differed since each component's SPI registers had to be looked up in its own datasheet.

### 5.4.1 Cell-Sleep

When we had learned more about the radio and felt confident in using MO Shell we started investigating Cell-Sleep. How to set up Cell-Sleep on a network node can be found in Appendix A.3. The usage of a thermal camera proved to be very useful in finding which components to focus on.

Since the radio cannot receive nor transmit anything during Cell-Sleep no considerations other than if it could return to active again was taken. This means that if the radio encountered a HW fault that could not be reset when a component was powered off, or if it could not be restarted properly, it was not included in our improved implementation. The test used to make sure it worked was to de-block the radio and return it to an operating mode and to send data. If it could go from our new implementation and back to operating mode, it was considered a success.

### 5.4.2 MIMO-Sleep mode

One of the first tasks that we had to do was to figure out which branch was turned off when the MIMO-Sleep feature was active. At first, this was done when the radio was assembled, and the only way of how to do it was with the use of software commands. This method gave unreliable results as the branches were named 0, 1, A and B, and several sources we found were inconclusive of which was which. To be sure, we had to operate the radio opened and observe with a thermal camera to see which branch, and which components were powered off.

When knowing which branch was turned off, the radio was connected to three UEs which were controlled with LiNS. To send data, in form of TCP streams, to and from the UEs the tool iPerf was used. The reason for attaching UEs to the radio and communicating with them was to see if, when powering off components or using clock gating, the UEs would still be able to communicate.

When investigating MIMO-Sleep when the radio was opened we had to, as mentioned earlier, lower the output power significantly. The reason for this was that the shields on the PCB board that are supposed to protect against RF exposure had to be removed so that we could see the components through the thermal camera. The improved feature was implemented with a script running MO shell and SPI commands.

### 5.4.3 Micro-Sleep Tx

When it comes to Micro-Sleep Tx several tests were made to understand how the feature works. Due to the limited time the radio was operated opened no further improvements were achieved. However, by studying the datasheets for the components in the Tx chains, a few of them were found suitable to be included in the feature due to their wake-up times.

## 5.5 Energy Model

To find power consumption values for the radios used in the model, the Ericsson tool PowerCalc was used. For Radio 2217 we used our own measurements. The measurements were done with the measurement setup described in Section 5.2 earlier where our radio was connected to a real base station and real UEs to provide load in the site.

The model configuration was written in Matlab as well as all calculations and plotted graphs. In Appendix C and D, coefficients for the polynomials and pseudo code for the algorithms used to calculate energy consumption with and without power save features are presented.

# Chapter 6
# Results

The first part of this chapter presents results of power savings for radio 2217 in different operating modes. The values presented here have all been taken from measurements during running the radio opened with an output power of 1 mW. Some of the components listed in the tables that are noted with an * are the ones that were not successfully implemented in the features but could prove to be interesting for future studies.

The second part presents results from our network model. As mention earlier the results are based on both measurements from PowerCalc and theoretical analysis.

## 6.1 Cell Sleep

The existing Cell Sleep feature consumes around 55.5 W when active. Among the commands for controlling the radio there was a power save command that was found for the Rx-branch. When using it while still having the Cell Sleep feature active the power consumption comes down to around 48.7 W. This implementation had been done by an Ericsson team conducting a power save study on the radio before our thesis work started. The implementation was however not implemented in Cell-Sleep.

The achieved improvements from our implementation of the feature resulted in reductions down to 35.44 W. In Figure 6.1 the transition from the existing Cell-Sleep to the new Cell-Sleep is shown. The total savings are approximately 19.87 W, which is a 36 % reduction in power consumption compared to the implemented Cell-Sleep. The implementations and the savings can be seen in Table 6.1. In Table 6.2 the components powered down are listed. The script for our implementation of Cell-Sleep can be found in Appendix A.1. All parts of the Rx block with the exception of the ADC had been powered off in Ericsson's improved implementation.

In the implementation with the lowest power consumption, the TOR LO, LTU clocks for TOR ADC, RX ADC, Digital Clocks and GSYNC was turned off. We did not succeed in turning on these again and had to restart the radio.

In Figure 6.2 a comparison between the power consumption of implemented Cell-Sleep, Ericsson-improved Cell-Sleep, our proposed Cell-Sleep and the last one, the lowest achieved Cell-Sleep. The lowest achieved power consumption was an average of 32.85 W. The heat signature in thermal camera did not change visibly compared to our proposed version. This implementation required us to restart the radio to be able to enable the cell again.

**Table 6.1:** Cell-Sleep improvement

| | Existing | Ericsson-improved | Improved | Lowest |
|---|---|---|---|---|
| Power | 55.31 W | 48.68 W | 35.44 W | 32.83 |
| Savings (W) | | 6.63 | 19.87 | 22.48 |
| Savings (%) | | 11.99 | 35.92 | 40.64 |

**Table 6.2:** Components powered down during Cell-Sleep. Components marked with * were not successfully implemented.

| Block | Components |
|---|---|
| Tx low | Modulator ASICs, DACs |
| TOR module | TOR ADCs |
| Rx front-end | Bypassed LNA |
| AIB | VSWR synth |
| iWarp 3.50 | Misc Clock (reg) |
| Rx | Rx ADC, LNA, IF ASIC, Mixer, VGA |
| PLL synth | Rx LO, TOR LO* |
| LTU | LTU clocks* |

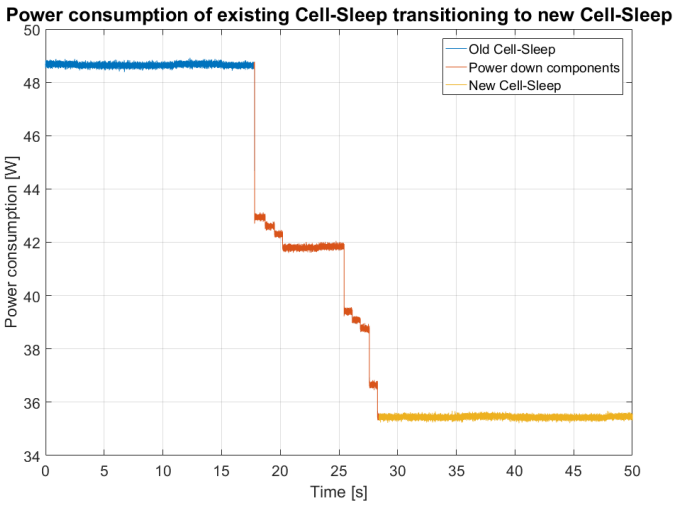


**Figure 6.1:** Transition from old blocked cell to our new implementation.

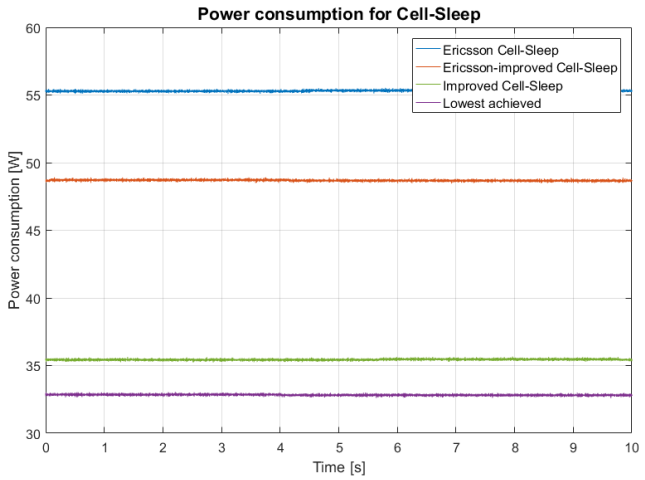


**Figure 6.2:** Power consumption comparison between the different implementations of Cell-Sleep.

### 6.1.1 Thermal images of Cell-Sleep

In Figure 6.3 the thermal image of the current Cell Sleep feature is shown. The RX-branch and the modulator ASICs are turned on, despite the RX-branch having an implemented power save in the software.

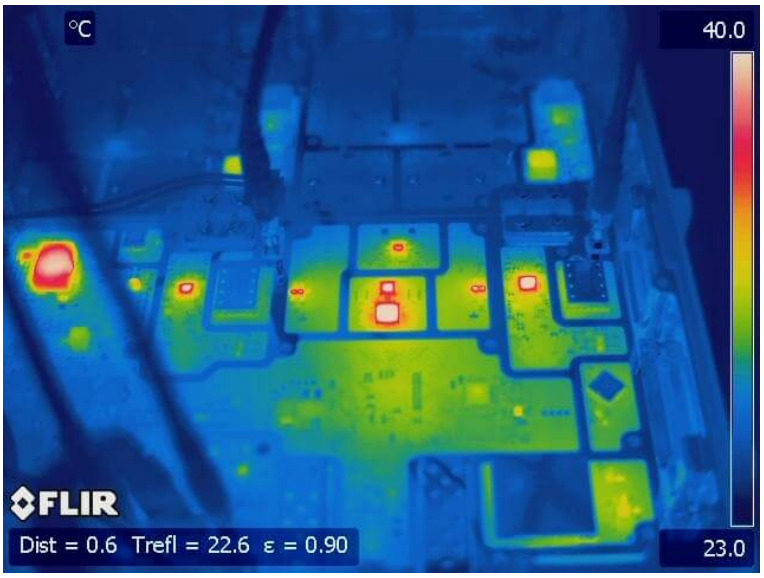


**Figure 6.3:** Thermal image during implemented Cell Sleep

In Figure 6.4 the thermal image of the implemented Cell Sleep feature is shown. The RX-branch is turned off. In Figure 6.5 our implementation of Cell-Sleep is shown. Notice how most components are turned off. The bright spot to the left and the two bright spots in the upper part of the photo are DC-DC-coils. Also notice that the heat signature has decreased significantly compared to the old implementation.

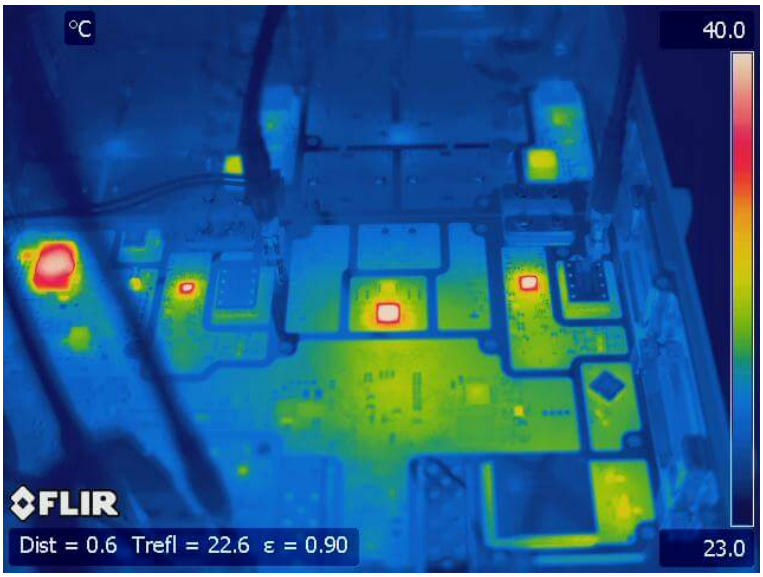


**Figure 6.4:** Old blocked cell. Ericsson improved Cell Sleep but not implemented.

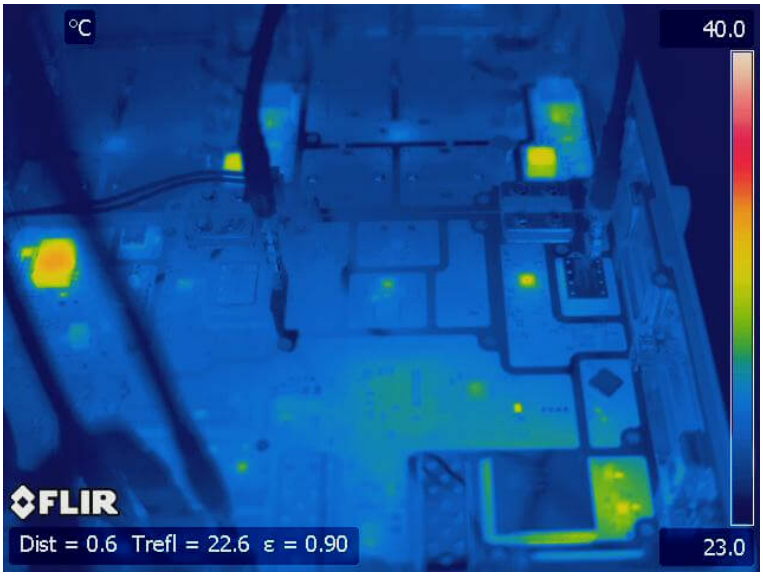


**Figure 6.5:** New Blocked cell. Our proposed new Cell Sleep.

## 6.2 MIMO-Sleep

When investigating MIMO-Sleep we found that the implementation that turned of the B-branch had a limitation in the way the hardware was built that made it harder to save power. This lead us to try to manually implement a new MIMO-Sleep that powered off the A-branch instead. This was successfully done and the new implementation was able to communicate and retain UEs the same way as the old implementation, as can be seen in Figure 6.6. The new implementation also saved more power than the already implemented MIMO-Sleep. A comparison between the different MIMO-Sleep implementations can be seen in Table 6.3. The components and clocks turned off can be found in Table 6.4. The script used to enable our proposed MIMO-Sleep can be found in Appendix A.2.

**Table 6.3:** MIMO-Sleep improvement

| | Existing | Improved Existing | New MIMO-Sleep | Proposed SISO |
|---|---|---|---|---|
| Power | 81.97 W | 80.45 W | 79.20 W | 76.26 W |
| Savings (W) | | 1.52 | 2.77 | 5.72 |
| Savings (%) | | 1.86 | 3.38 | 6.97 |

**Table 6.4:** Components powered down during MIMO-Sleep, Components marked with * are included in the SISO-implementation.

| Blocks | Components |
|---|---|
| Tx | PA, peak- and main-driver |
| TOR | ADC |
| Tx low | Modulator ASIC |
| iWarp 3.50 | Clock gating |
| Rx | IF ASIC:A*, VGA:A*, LNA2:A*, LNA1:A* |

A comparison plot between the different MIMO-Sleep (and SISO-implementation) is shown in Figure 6.7.

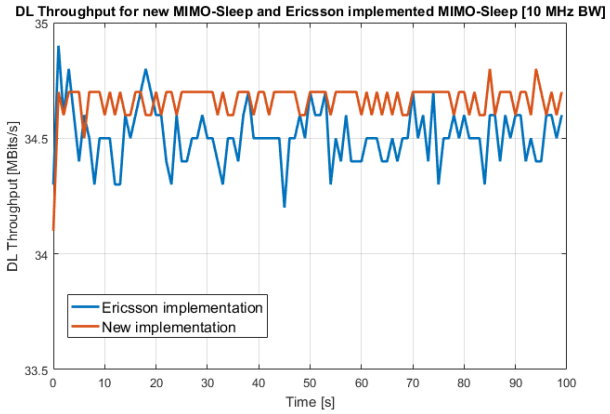


**Figure 6.6:** Throughput of implemented MIMO-Sleep and new MIMO-Sleep.

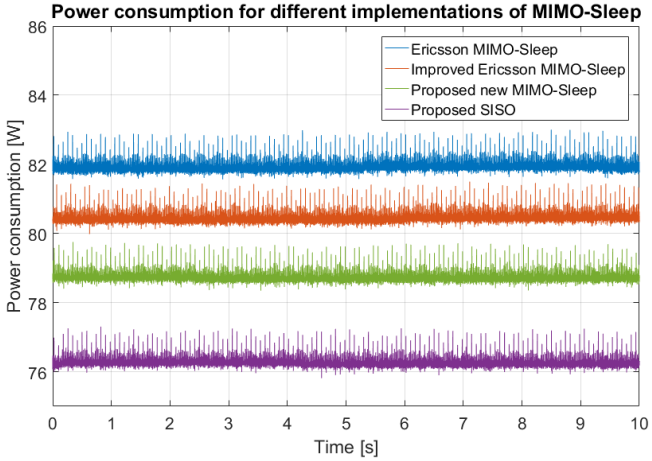


**Figure 6.7:** Comparison of power consumption for the different implementations of MIMO-Sleep.

### 6.2.1 Measurements at 2x40 W output power

An earlier version of the improved MIMO-Sleep that did not include all the components powered off in the final version was tested when the radio was assembled and at 80 W output power. This version did not include the TOR ADC. The improved implementation lowered the power consumption by 3.2 W. This is a reduction in power consumption by 3.39 %. A plot of the power consumption can be seen in Figure 6.8.

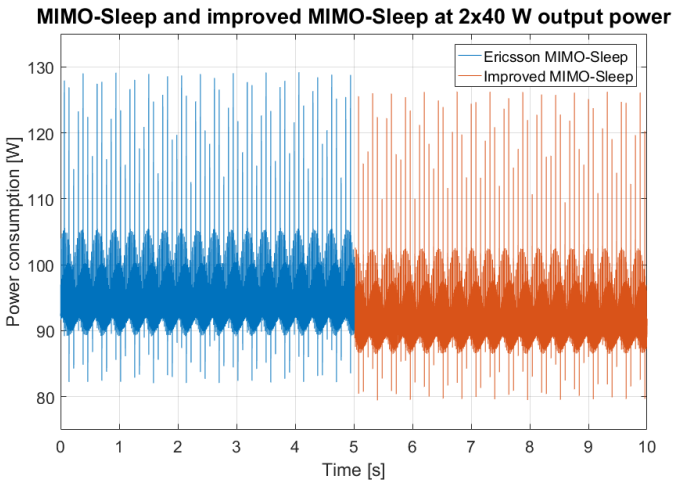


**Figure 6.8:** Implemented MIMO-Sleep and early version of improved MIMO-Sleep at 2x40 W (80 W) output power.

### 6.2.2 Thermal images of MIMO-Sleep

Thermal images were taken to identify differences between Ericsson-implemented MIMO-Sleep and our implementation MIMO-Sleep. The Ericsson-implemented MIMO-Sleep can be seen in Figure 6.9 and our proposed implementation can be seen in Figure 6.10.

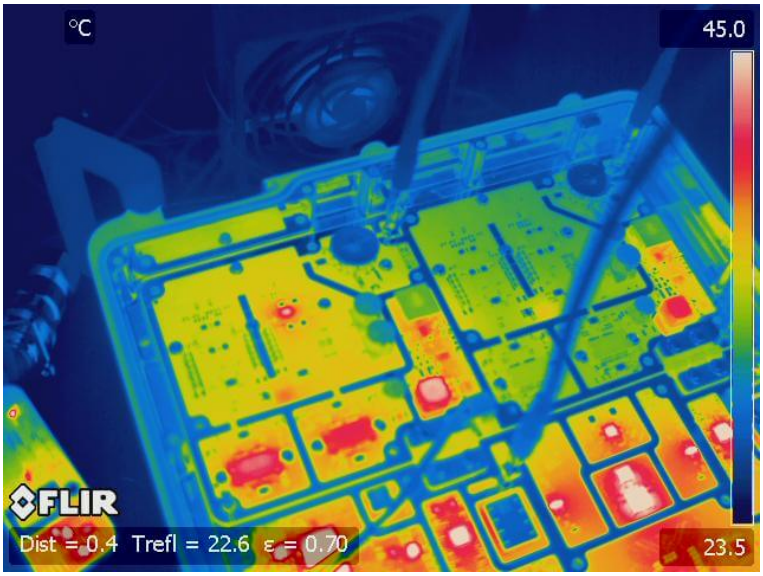


**Figure 6.9:** Ericsson implementation of MIMO-Sleep. The B-branch is turned off.

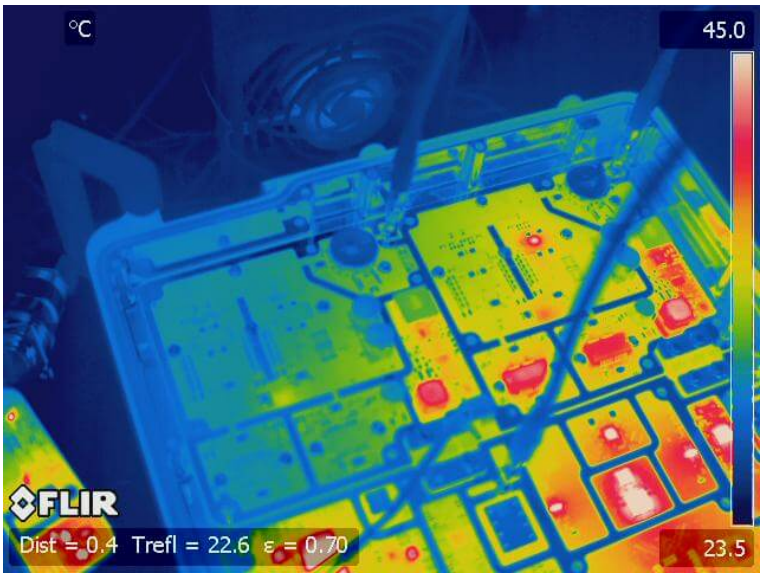


**Figure 6.10:** Our implementation of MIMO-Sleep. The A-branch is turned off.

## 6.3 Micro Sleep TX

Unfortunately due to limited time and problems acquiring the correct cables and antenna contacts no work was done on Micro-Sleep Tx with the exception of finding possible components to be included in the feature. A table presenting possible components can be seen in Table 6.5.

**Table 6.5:** Components powered down during MIMO-Sleep, *SISO

| Blocks | Components |
|---|---|
| Tx low | DACs |
| TOR | ADC |
| Rx | LNA, RF VGA, IF ASIC |

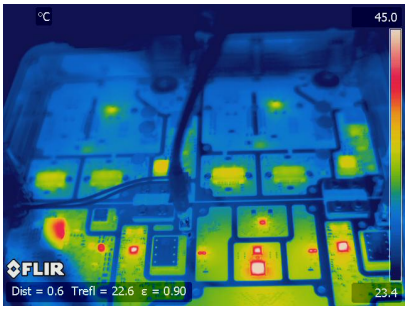


**Figure 6.11:** Micro Sleep TX disabled.

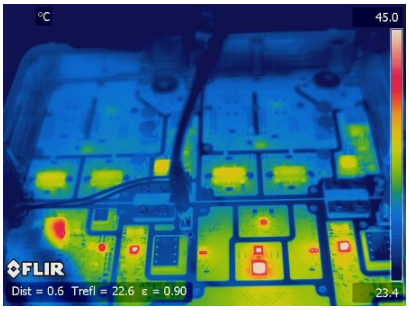


**Figure 6.12:** Micro Sleep TX enabled. Heat dissipation from the PA are clearly lower.

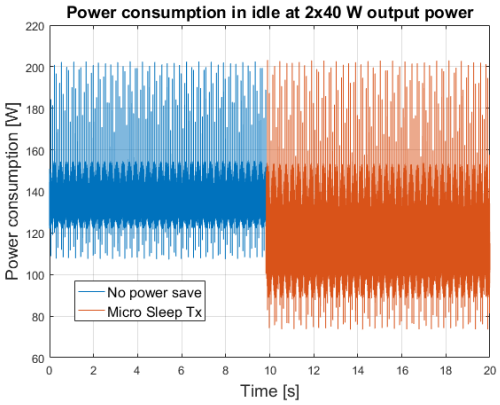


**Figure 6.13:** Idle power consumption on Radio 2217 with and without Micro Sleep Tx.

## 6.4 Energy Model

In Table 6.7 the energy consumption and savings are presented. Figure 6.14 shows the total energy consumption per year before the hardware substitution and Figure 6.15 shows result after the substitution. The colored bars represents the different power save features (PSF). In Appendix E the energy consumption results for each site configuration is shown.

**Table 6.6:** Savings compared to existing hardware with no power save features activated.

| Hardware | Savings with PSF |
|---|---|
| Existing | 28 % |
| Upgraded | 57 % |

**Table 6.7:** Model comparison

| | No PS | +$\mu$Sleep | +LESS | +HOPE | +MIMO-Sleep | + Cell-Sleep |
|---|---|---|---|---|---|---|
| Energy before (GWh) | 289 | 266 | 260 | 230 | 212 | 209 |
| Energy after (GWh) | 177 | 152 | 147 | 140 | 127 | 125 |

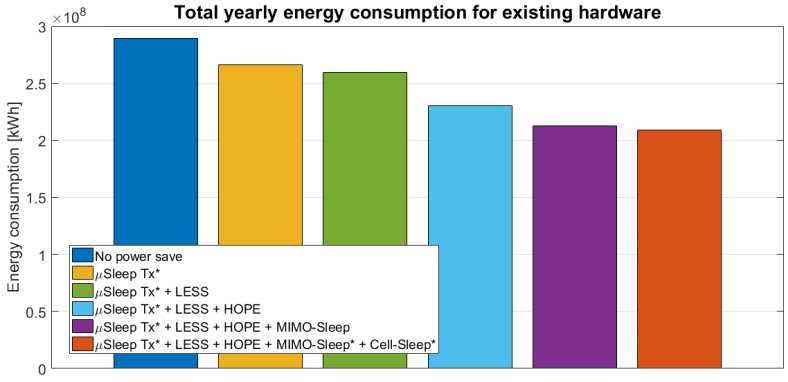


**Figure 6.14:** Yearly energy consumption with existing radio hardware.

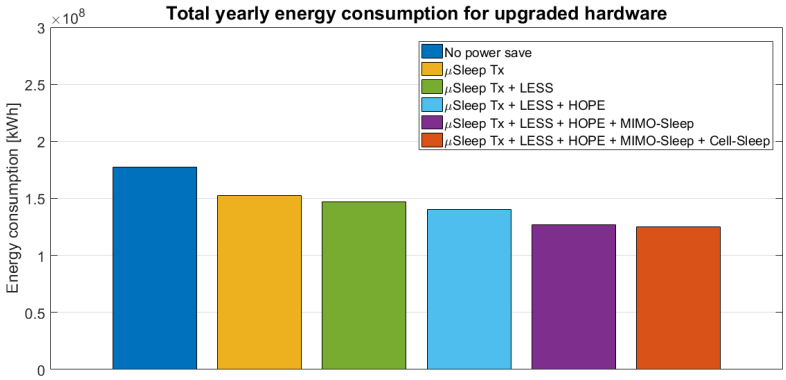


**Figure 6.15:** Yearly energy consumption with upgraded radio hardware.

The bar graph in Figure 6.16 shows the cost savings in SEK for the network calculated in the model. With old hardware, the added power save features resulted in reduced monetary costs of 80 MSEK. When substituting all radio units with new hardware the total savings per year amounted to 164 MSEK. What is essential about this figure is not the values themselves, but rather the impact newer hardware directly has on the energy efficiency and the energy cost of a mobile network.

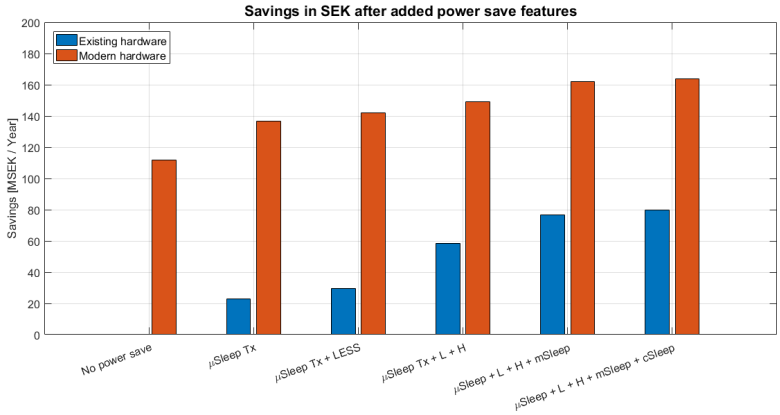


**Figure 6.16:** Plot of savings in SEK for both hardware configurations compared to the old hardware configuration with no power save.

### 6.4.1 Carbon footprint

When comparing the different configurations of existing and upgraded hardware it is interesting to look not only at the energy consumption, but also the reduced amount of diesel and greenhouse gas emissions. In Table 6.8 the comparison can be seen.

**Table 6.8:** Comparison in diesel consumption between the existing and upgraded hardware for 17.8 % of the sites considered to be off-grid.

| Hardware | Diesel (million liters) | $CO_2$ (tonnes) |
|---|---|---|
| Existing | 14.6 | 37960 |
| Upgraded | 6.3 | 16380 |
| Saving | 8.3 | 21580 |

To provide an alternative perspective an example with cars can be used. The average distance traveled for private cars is estimated to be around 23 000 km and the average fuel consumption in liters is 4.89 per 100 km [22]. This equates to 1124.7 liters diesel per year for a private car. With these figures, the amount of diesel needed to power 17.8 % of our network with existing hardware could run 12981 cars for a whole year. With upgraded hardware this figure changes to 5601 cars.

# Chapter 7
# Discussion

## 7.1 Power saving for radio 2217

It should be noted that since the output power was set to only 1 mW, the results in terms of power consumption savings are a bit different from when we run the radio assembled with 2x40 W output power. For example, with 2x40 W output power we had a reduction of 3.2 W in MIMO-sleep compared to 2.77 W when the radio was opened. We also noticed a slightly higher power consumption in Cell-Sleep when the radio was assembled.

A reason for the difference in power consumption could possibly be that the temperature of the components are slightly higher when the radio is assembled and this might produce more leakage in the micro circuits.However, as presented in the results for MIMO-Sleep, the relative difference between both measurements are around the same, suggesting that the percentage decrease presented can be applied whether the radio is assembled or opened.

Although it was not shown in this study it should be noted that the power features might have other positive effects such as lower heat dissipation causing auxiliary systems like air conditioning and such to consume less power and also extend the lifetime of the radio unit and other units. This will need to be further investigated in the future.

## 7.2 Cell-sleep

As expected this is the feature that enables most components to power down because the radio neither transmits nor receives any data or control signaling. As can be seen in the results several components are powered down, both on the PA board and the TRX board.

As presented in the results section of Cell Sleep, there is a possibility to save even more power by turning off LO signals and clock signals from the LTU. However, this was not possible for us without triggering HW faults on the radio, and also causing forced restarts in some cases. Some of the alarms that were raised could actually be cleared in the radio after powering on the component that caused

it. Even though the alarm was still present on the baseband alarm list, and could not be cleared since our baseband software version was secure, ie. not allowing certain commands, the radio was able to return to active mode and receive and transmit data. When testing on another "unlocked" baseband it was possible to clear the alarm.

The LTU has several clock signals that are able to be powered down. These lower the power consumption by around 1.5 W. We were not successful in resetting the clock signals and to return the radio to active mode afterwards though. The reset-register in the LTU forces the radio to restart since it seems to momentarily restart the LTU causing the iWarp 3.50 to lose clocking.

It could be discussed whether those failures are actually real faults which are unable to be recovered from or just predefined in the software. The reason for pointing this out is that in order to power down the X component the fault alert in the radio was ignored, even though the alarm in the baseband log could not be deleted.

## 7.3 MIMO-Sleep

As presented in the results, we were able to achieve a reduction in power consumption by around 3.4 % compared to the Ericsson-implementation. This was done by changing the branch that should power off to A instead of B, resulting in additional available to turn off. The reason for doing this was that in the hardware implementation it was seen that the modulator ASICs are connected in a daisy chain. The ASIC on the B-branch receives a PLL which is then fed to the ASIC on the A-branch, resulting in that if the ASIC on the B-branch was powered off the ASIC on the A-branch would lose its PLL signal. This caused both modulator ASICs to lose functionality and hence disrupting all downlink transmissions. It also resulted in an automated restart of the radio.

A part of this section has been removed due to confidentiality.

A 3.4 % reduction at a first glance, perhaps does not seem that significant compared to a 35.9 % reduction for the Cell-Sleep case. However, MIMO-Sleep is a power save feature that sees more possible usage areas and does not impact the network in such a severe way as Cell-Sleep. MIMO-Sleep only halves the throughput in downlink compared to Cell-Sleep which disrupts all traffic to in cell. This enables MIMO-Sleep to be active a lot more often than Cell-Sleep. Given that MIMO-Sleep could potentially be used a lot more and it could effectively be used on hundreds of thousands, if not millions of radios the potential power save could be substantial.

### 7.3.1 SISO-Sleep

Since the RX-chain is implemented in (almost) two branches, some components on one chain can be turned off to save more power. This could be viable in very

rural areas where the site experiences extremely low load during certain hours. Unfortunately, the radio restarted itself after around 10 minutes of operation when in SISO-mode. We were unable to find out the reason for the restarts.

## 7.4 Micro-Sleep

Unfortunately more time was needed in order to improve the Micro-Sleep Tx feature since we had some trouble acquiring the needed cables to run the radio opened. However several suggestions of improvements were considered.

At first, more components at the Tx branch could be powered down if their wake-up times are short enough. The components in the Tx-chain that could be powered down are unfortunately not that power consuming so the reduction would not be that great compared to the already implemented version. Secondly it should be investigated whether some components in the Rx chain could be powered down as well, for instance one or both of the LNA. The UL time-frequency grid is different compared to the DL, so the possibilities could be reduced.

It should be noted that it might not be possible to implement much more power save features during Micro-Sleep Tx since the radio is an FDD radio, which means that it transmits and receives during the same time.

In case of TDD there is a certain guarantee that there will be time slots where the receiver will not be available and this could mean a possibility to activate Micro-Sleep in the receiver chain without much effort. It should also be possible to turn off more components and possibly some clock or LO signals in both the Tx and Rx chain since startup times can be much slower compared to FDD.
Another improvement would be to combine other power saving features such as Less and HOPE with the feature.

## 7.5 Energy Model

The network we modeled was a quite large network with 147 000 radios in the configuration with old hardware and 122 000 with new hardware. The reason for the lower amount of radios in the model with new hardware is because the configuration on site configuration number 3 has changed from six 1 TRX radio to one 2 TRX radio in a PSI-configuration.

The reason we chose to have four different site configuration was to be able to assess how power save features affect different kind of models of radio units. From the discussions with people working with energy analytics at Ericsson it was also made clear that real networks often have a variety of different radio models to suit different needs in the network. The needs can vary from which bands should be supported and how much output power is needed to how many antennas and so forth. In our model we have used eight different radio units, where four are characterized as old hardware and four as new hardware that substitutes the old

units in the modern model. The substitution choices comes from Ericsson internal substitution plans and are chosen in the model because of that.

The other power save features used are estimated after discussions with people working on them. LESS and HOPE for example are still being trialed so there were not much information available about definite values of how much power they save. There are also different values for Micro-Sleep Tx and HOPE for some radios. This is because some radios have different hardware implementations which changes the effect of the feature on the power consumption [ericsson internal].

With regards to the duration enabling MIMO-Sleep we estimated that sites with a low average daily load, chosen as below 12 %, could sleep for 10 hours and have normal operation during the rest of the day. Since the load typically is very low during the night and during some other times during the day we felt that 10 hours were a reasonable duration to enable it. MIMO-Sleep switches on and off very fast [internal], further convincing us that it could be enabled for short periods during the day when the load momentarily is low. For sites with a daily average load higher than 12 % we felt more restricted in the use of MIMO-Sleep and chose to use the default values. We believe that this is a low estimate and could probably be increased to include more hours. The default value was chosen because we tried to not overestimate the power saving capability. For Cell-Sleep we chose to enable it for six hours if the average daily load was under 8 %. This, we believe, was also a low estimate and could probably be increased by a couple of hours. The cut-off load for when we do not enable Cell-Sleep anymore is also a low estimate and could probably be increased to be more in line with the cut-off for MIMO-Sleep.

The main problem with estimating and creating algorithms for energy consumption of sites is that it is crucial knowing where the site is placed and how the traffic in the area behaves. For instance, a site could be placed at a sports arena and have several bands to deliver capacity to all visitors during events, but when there is no event the radios would then be idle or with low traffic. Some of the capacity bands could in this example enter Cell-Sleep for very long durations when no big events are scheduled.

One thing that needs to be kept in mind when analyzing the model is that the power consumption from other RAN related products such as the baseband, cooling equipment etc. are not included. This study was mainly aimed to show how the power consumption of a network could be reduced by just improving the energy efficiency of radio units.

## 7.6 Carbon footprint

Any decrease of power consumption at the site directly contributes to less fuel used and less greenhouse gases released, as well as cost reductions of buying diesel and refueling less often. This leads to the possibility of powering off-grid sites with other energy sources instead of diesel. An example is the use of solar power to

power the base station. This has already been tested successfully by Ericsson [23] but could be used more widely if energy consumption decreases.

# Chapter 8

# Conclusion and Future Work

In this thesis work it was showed that existing power save features could be improved further. Over the course of a few months we were able to reduce the power consumption of Cell-Sleep by 36.0 % and MIMO-Sleep by 3.4 %. More power save could presumably be possible on both features by using more energy optimized hardware and further software implementations to control components. In our work we only studied one type of radio unit but we strongly believe that other radio units could benefit from this type of study, and that similar reductions in power consumption can be achieved. From the measurements, it was clear that power consumption did not scale well with the load on the radio. Further research should be done in order to enable better scalability between power and load.

It was also showed in the energy model how big of an impact modern hardware and power save features has on the overall energy consumption in the network. This is a conclusion that can be used to show operators the gain of modernizing hardware and enabling power save features. From the model it can also be seen that hardware is becoming more and more energy efficient and that there is ongoing work that aims to lower the power consumption of the radio units. A lot of the components on the radio have power save features and are controllable through SPI.

More work can definitely be done with regards to the energy model. Future studies of this type would benefit from having actual measurements for the different power save features for all radio units as well as using real traffic profiles.

It is important to note that the radio unit should not be the only blame for high energy consumption. LTE is a communication standard that often transmits control signals, forcing the radio to consume power. Thus, less control signaling and longer durations where the radio does not have to transmit are key to improve energy efficiency. This is something that is planned in 5G. For future works, we believe that hardware designers and radio standard implementers should work together to find better solutions to save more power.

# References


[1] Cisco White paper, *Cisco Visual Networking Index: Global Mobile Data Traffic Forecast Update, 2016–2021, 2017*

[2] Ericsson, *Ericsson Mobility Report, November 2015*

[3] The Evolution of Mobile Telecommunications - Qualcomm

[4] Proposal for Candidate Radio Interface Technologies for IMT-Advanced Based on LTE Release 10 and Beyond (LTE-Advanced) - T. Nakamura, http://www.3gpp.org/IMG/pdf/2009_10_3gpp_IMT.pdf,2017-03-04

[5] LTE ue-Category 3GPP http://www.3gpp.org/keywords-acronyms/1612-ue-category,2017-09-10

[6] The LTE Network Architecture - Alcatel, http://www.cse.unt.edu/~rdantu/FALL_2013_WIRELESS_NETWORKS/LTE_Alcatel_White_Paper.pdf,2017-06-01

[7] E. Dahlman, S. Parkvall, J. Sköld, *4G LTE-Advanced Pro and The Road to 5G*

[8] Ericsson internal

[9] G. Lindell, *Lecture notes on OFDM in course ETTN15, Lund University, 2016*

[10] Xiurong Bao, "Matlab simulation and performance analysis of OFDM system", *Computer Science and Information Processing (CSIP), 2012*

[11] G. Lindell, *Introduction to Digital Communication*

[12] MIMO – Diversity and Spatial Multiplexing, http://www.gaussianwaves.com/2014/08/mimo-diversity-and-spatial-multiplexing/

[13] Ericsson internal

[14] Bad-Grid Solution, http://www.deltaelectronicsindia.com/products/telecom-bad-grid.html,2017-06-10

[15] GREEN POWER FOR MOBILE BI ANNUAL REPORT, 2014, https://www.gsma.com/mobilefordevelopment/wp-content/uploads/2014/08/GPM_August2014_FINAL.pdf,2017-03-15

[16] GSMA, https://www.gsma.com/mobilefordevelopment/wp-content/uploads/2012/05/Energy-for-the-Telecom-Towers-India-Market-Sizing-and-Forecasting-September-2010.pdf,2017-04-13

[17] DEFRA, "Act on CO2 Calculator: Data, Methodology and Assumptions Paper", V1.2, Aug. 2008.

[18] Table 8.2. Average Tested Heat Rates by Prime Mover and Energy Source, 2007 - 2015, https://www.eia.gov/electricity/annual/html/epa_08_02.html,2017-06-08

[19] Ericsson Review, 2014-02, *Radio network energy performance: Shifting focus from power to precision* https://www.ericsson.com/assets/local/publications/ericsson-technology-review/docs/2014/er-radio-network-energy-performance.pdf,2017-02-17

[20] Ericsson internal document on frequency bands

[21] FLIR P-Series Infrared Cameras, http://www.flir.com/instruments/display/?id=60087,2017-06-10

[22] http://www.cso.ie/px/pxeirestat/statire/temp/20176161232457296 26SEI07.htm,2017-05-29

[23] The Green Mobile Award, https://www.globalmobileawards.com/green-mobile-award/,2017-06-15

# Appendix A
# MO Shell Scripts

This appendix has been removed due to confidentiality.

# Appendix B
# AT-commands

In this appendix the AT-commands used to control the UEs are listed.

```
at+cfun=4 - Enables flight mode
at+cfun=4,1 - Restarts the UE in flight mode
at+cfun=8 - Enables LTE
at*enap=1 - Enables data
```

Appendix C

# Coefficients and power save estimates

This appendix has been removed due to confidentiality.

# Appendix D
# Algorithms

Algorithm for no power save feature: Algorithm for Micro-Sleep Tx: Algorithm for

**Algorithm 1** No feature

1: $powernf \leftarrow 0$ ▷ initialize variable
2: $distribution \leftarrow nbrOfSites \cdot distr$ ▷ load distribution
3: **for** length of distribution array **do**
4: $nbrRadios \leftarrow distribution(i) \cdot$ configured radios
5: $powernf \leftarrow powernf + nbrRadios \cdot f_{nofeat}(prbLoad)$
6: **end for**
7: $powernf \leftarrow powernf \cdot 24 \cdot 365.25/1000$ ▷ Calculate yearly kWh

**Algorithm 2** $\mu$Sleep

1: $poweru \leftarrow 0$ ▷ initialize variable
2: $distribution \leftarrow nbrOfSites \cdot distr$ ▷ load distribution
3: **for** length of distribution array **do**
4: $nbrRadios \leftarrow distribution(i) \cdot$ configured radios
5: $poweru \leftarrow poweru + nbrRadios \cdot f_{\mu}(prbLoad)$
6: **end for**
7: $powernf \leftarrow powernf \cdot 24 \cdot 365.25/1000$ ▷ Calculate yearly kWh

Micro-Sleep Tx with LESS: Algorithm for Micro-Sleep Tx with LESS and HOPE: Algorithm for Micro-Sleep Tx, LESS and MIMO-Sleep combined: Algorithm for Micro-Sleep Tx, LESS, MIMO-Sleep and Cell-Sleep combined:

**Algorithm 3** $\mu$Sleep + LESS

1: $powerul \leftarrow 0$ ▷ initialize variable
2: $distribution \leftarrow nbrOfSites \cdot distr$ ▷ load distribution
3: **for** length of distribution array **do**
4: $nbrRadios \leftarrow distribution(i) \cdot$ configured radios
5: $powerul \leftarrow powerul + nbrRadios \cdot f_{\mu l}(prbLoad)$
6: **end for**
7: $powerul \leftarrow powerul \cdot 24 \cdot 365.25/1000$ ▷ Calculate yearly kWh

**Algorithm 4** $\mu$Sleep + LESS + HOPE

1: $powerhul \leftarrow 0$ ▷ initialize variable
2: $distribution \leftarrow nbrOfSites \cdot distr$ ▷ load distribution
3: **for** length of distribution array **do**
4: $nbrRadios \leftarrow distribution(i) \cdot$ configured radios
5: $powerhul \leftarrow powerhul + nbrRadios \cdot f_{h\mu l}(prbLoad)$
6: **end for**
7: $powerhul \leftarrow powerhul \cdot 24 \cdot 365.25/1000$ ▷ Calculate yearly kWh

**Algorithm 5** $\mu$Sleep + LESS + HOPE + MIMO-Sleep

1: $powerhulm \leftarrow 0$ ▷ initialize variable
2: $distribution \leftarrow nbrOfSites \cdot distr$ ▷ load distribution
3: **for** length of distribution array **do**
4: $nbrRadios \leftarrow distribution(i) \cdot$ configured radios
5: **if** prbLoad(i) $\leq 12$ **then**
6: $powerhulm \leftarrow powerhulm + 10/24 \cdot nbrRadios \cdot f_{h\mu lm}(prbLoad)$
7: $+ 14/24 \cdot nbrRadios \cdot f_{h\mu l}(prbLoad)$
8: **else**
9: $powerhulm \leftarrow powerhulm + 3/24 \cdot nbrRadios \cdot f_{h\mu lm}(prbLoad)$
10: $+ 21/24 \cdot nbrRadios \cdot f_{h\mu l}(prbLoad)$
11: **end if**
12: **end for**
13: $powerhulm \leftarrow powerhulm \cdot 24 \cdot 365.25/1000$ ▷ Calculate yearly kWh

**Algorithm 6** $\mu$Sleep + LESS + HOPE + MIMO-Sleep + Cell-Sleep

$powerchulm \leftarrow 0$ ▷ initialize variable
$distribution \leftarrow nbrOfSites \cdot distr$ ▷ load distribution
**for** length of distribution array **do**
    $nbrRadios \leftarrow distribution(i) \cdot$ configured radios
    $nbrCapRadio \leftarrow$ number of Cell-Sleep radios
    **if** $prbLoad(i) \leq 8$ **then**
        $powerchulm \leftarrow powerchulm + nbrCapRadio \cdot (6/24 \cdot Blocked$
                $+ 6/24 \cdot f_{h\mu lm}(prbLoad) + 12/24 \cdot f_{h\mu l}(prbLoad)$
                $+ 10/24 \cdot nbrOfRadios \cdot f_{h\mu lm}(prbLoad)$
                $+ 14/24 \cdot nbrOfRadios \cdot f_{h\mu l}(prbLoad)$
    **else if** $8 < prbLoad(i) \leq 12$ **then**
        $powerchulm \leftarrow powerchulm + 10/24 \cdot nbrRadios \cdot f_{h\mu lm}(prbLoad)$
                $+ 14/24 \cdot nbrRadios \cdot f_{h\mu l}(prbLoad)$
    **else**
        $powerchulm \leftarrow powerchulm + 3/24 \cdot nbrRadios \cdot f_{h\mu lm}(prbLoad)$
                $+ 21/24 \cdot nbrRadios \cdot f_{h\mu l}(prbLoad)$
    **end if**
**end for**
$powerhulm \leftarrow powerchulm \cdot 24 \cdot 365.25/1000$ ▷ Calculate yearly kWh

# Appendix E

# Power consumption on the different site configurations

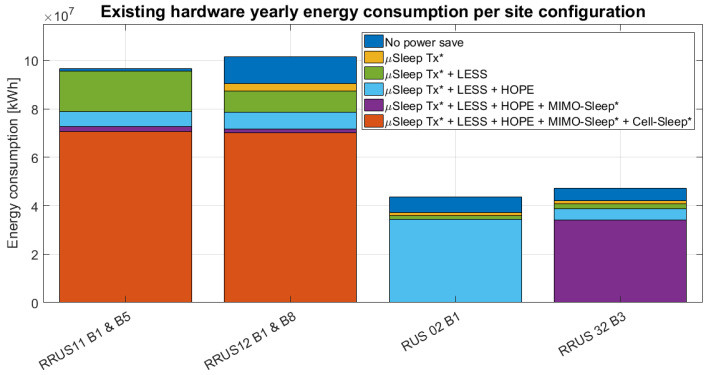


**Figure E.1:** Energy consumption for each site configuration with existing radio hardware.

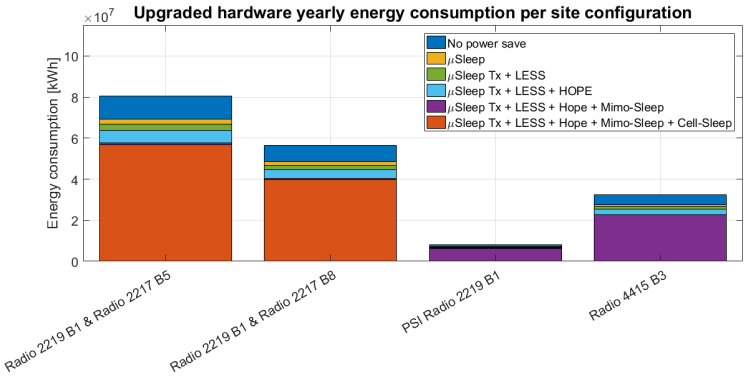


**Figure E.2:** Energy consumption for each site configuration with upgraded radio hardware.